AN INSTRUMENTED, MICROPROCESSOR-ASSISTED RESIDENTIAL ENERGY AUDIT

R. C. Sonderegger, D. T. Grimsrud and D. L. Krinkel
Energy Performance of Buildings Group
Lawrence Berkeley Laboratory
University of California
Berkeley, CA 94720, USA

Abstract

An energy audit has been developed to determine economically optimal retrofits for residential buildings, based on actual, on-site measurements of key indices of the house. Measurements are analyzed on a microprocessor and retrofit combinations compatible with minimum life-cycle cost and occupant preferences are then determined.

A novel element in this audit is the determination of monthly values of air infiltration derived from measurement of the "effective leakage area" of the house combined with local weather, terrain and the house leakage distribution.

Heating and cooling loads are computed on the basis of "dynamic degree-days" that make use of the time constant of the house, monthly values of internal and solar gains, and infiltration, and permit an accurate evaluation of potential energy savings. These two novel calculation procedures are described in the context of the audit.

Introduction

We are currently developing an energy audit procedure for determining the economically optimal retrofit package for a given residential building. This audit is a microprocessor-based, interactive, site- and house specific package addressing conservation and solar measures. The audit is aimed at utility companies, state energy offices and/or private energy contractors. In the following section we will briefly describe the main features of this audit. We will subsequently focus exclusively on two novel calculation procedures employed by the audit: a dynamic load evaluation procedure and a method to estimate air infiltration from pressurization results.

The work described in this report was funded by the Office of Buildings and Community Systems, Assistant Secretary for Conservation and Solar Applications of the U.S. Department of Energy under contract No. W-7405-Eng-48.

Overview of the audit

Before the actual audit visit, past utility bills of the house and weather data are screened to obtain an "energy signature" for the house. Subsequently, two auditors visit the house. They note window types and measure dimensions, test the envelope for leakage with a blower door that pressurizes or depressurizes the house, identify leaks, plug the easy ones as they go and note the ones that are more difficult to repair. While one auditor measures furnace efficiency, checks water and air temperature settings, and estimates envelope R-values, the other auditor repairs air leaks, installs water heater insulation, changes the furnace air filter, calibrates the thermostat and, with the permission of the homeowner, installs a low-flow showerhead and resets the water heater thermostat.

At the conclusion of the physical inspection, all necessary data are collected and fed to the microprocessor. The microprocessor features a state-of-the-art interactive program that asks simple questions and provides further information on its questions when requested. The homeowner is present during this process and is encouraged to answer the questions either directly, or through the auditors. The auditors then help the homeowner decide on a suitable retrofit package. The program scans a master list of possible retrofits stored on a disk that includes conservation measures, such as insulation, storm and double-pane windows, insulating shutters, caulking and weatherstripping,

There is ample occasion for interaction between the homeowner and the program to insure that no optimized retrofit lists are produced with items unacceptable to the homeowner, and that the homeowner is educated on-site about the costs and benefits of retrofits. Of course, our cost estimates of all retrofit packages acknowledge that homeowners may do some retrofits themselves and hire a contractor to do others. At the conclusion of the visit, the auditor leaves behind specific detail information on the suggested retrofits. . vent dampers, replacement burners, and active and passive solar retrofits for space and water heating.

A dynamic heating and cooling load model with algorithms to calculate internal heat gains and solar gains is used to evaluate fuel savings. Special attention is given to the estimation of monthly average air infiltration rates, using a model correlating pressurization results with air infiltration under natural weather conditions.

In the following sections we will describe the dynamic load model and the algorithm used to estimate monthly air infiltration values.

Simulation of space heating energy consumption

Energy savings from all retrofit packages considered during the audit are estimated with a new, fast heating and cooling model. In this model, a house at any stage of retrofit is characterized by the following parameters: 1) heating and cooling system efficiency; 2) heat transmission coefficient; 3) air infiltration rate; 4) time constant; 5) solar aperture; 6) day and night thermostat setting; 7) day and night values of "free heat" (lights, appliances, people, ground losses). On the basis of these parameters, heating and cooling energy consumption is estimated on a monthly basis, using hourly temperatures and monthly averages of solar radiation.

In order to speed up the audit, a good part of these calculations are done in advance for a given city, and tabulated on a monthly basis, for many values of the house parameters. We call the quantities calculated in advance "dynamic degree-days." As the name indicates, dynamic degree-days take into account the dynamic response of a building and, for very light buildings with no thermostat setbacks, they assume values identical to conventional degree-days.

During the actual field audit, then, estimating monthly and yearly energy consumptions is reduced to: 1) calculating the appropriate values of the house parameters for a given retrofit configuration; 2) retrieving the entries corresponding to the set of house parameters from the table of pre-calculated dynamic degree-days; 3) multiplying these entries month-by-month by the conduction and heat loss coefficients and dividing the result by the heating or cooling efficiency.

This procedure is described schematically by the following equation, which expresses the monthly energy consumption for heating or cooling:

$$E = \frac{UA + Q\,\rho c}{\eta} DDD \qquad (1)$$

where: E is the monthly energy consumption (kWh/Mo);
UA is the overall heat transmission coefficient (kWh/^{o}C-day);
Q is the air infiltration rate (m^3/day);
ρc is the heat capacity of air at room temperature ($.335 \times 10^{-3}$ kWh/^{o}C-m^3);
η is the heating or cooling system efficiency;
DDD is the value of heating or cooling dynamic degree-days (^{o}C-day).

The values of the parameters in this equation change each month. Yearly heating and cooling consumptions are simply the sum of 12 monthly consumptions.

Dynamic Degree-Days

As with conventional degree-days, dynamic degree-days serve as climate quantifiers. Conventional degree-days for a particular month are calculated by summing the difference between an indoor reference temperature (in the U.S. typically 18.3 ^{o}C) and the average outdoor temperature for each day of the month. Days where this difference is negative are excluded. Recently, this definition has been extended to allow a variable indoor reference temperature in order to give proper credit to the improved utilization of "free heat" and solar gains in energy-efficient dwellings. We call these "Variable degree-days".[1] (A slightly different definition has employed by researchers at the University of Liège.[2])

The definition of variable degree-days reflects the fact that degree-days are both site- and house-specific. Two houses side-by-side may "see" a different number of degree-days. Dynamic degree-days extend the quantification of such house-specific factors. Specifically, dynamic degree-days can handle the dynamic characteristics of houses and, thus, thermostat setbacks.

In mathematical terms, monthly dynamic degree-days are calculated by integrating, hour-by-hour, the following differential equation:

$$C \frac{dT}{dt} = \eta E' + F + A\,S - (UA + Q\,\rho c)\,(T - TO) \qquad (2.1)$$

subject to one set of the following boundary conditions:

$$E' = 0 \text{ for } T > TS \quad \text{and} \quad 0 \leq E' \leq E'_{max} \text{ for } T \leq TS \quad \text{(heating)} \qquad (2.2)$$

$$E' = 0 \text{ for } T < TS \quad \text{and} \quad 0 \leq E' \leq E'_{max} \text{ for } T \geq TS \quad \text{(cooling)} \qquad (2.3)$$

where: t is the time (day);
T is the indoor temperature (^oC);
TO is the outdoor temperature (^oC),
TS is the thermostat setting (^oC);
C is the effective heat capacity of the house (kWh/K);
E′ is the heating or cooling energy consumption (kWh/day);
E'_{max} is the maximum heating or cooling system input capacity (kWh/day);
F is the free heat (kWh/day);
A is the solar aperture (m^2);
S is the solar flux on the south wall (kWh/day);

All other symbols have been defined earlier. To calculate the effective heat capacity of the house, C, we use the definition of "diurnal heat capacity",[3] which is the thermal mass exhibited by the house at 24 hour-oscillations of temperature and heat flow.

Generally, the thermostat setting is assumed to be reset twice every day. For purposes of our audit, the day is defined as the 16 hours between 6^{oo} and 22^{oo}, night is defined as the eight hours between 22^{oo} and 6^{oo} of the following morning. With the inclusion of thermostat setback, the calculation of dynamic degree-days becomes somewhat complicated. Before we continue, it is useful to introduce a time constant of the house, τ, and two temperature offsets, Z_d and Z_n, for day and night:

$$\tau = \frac{C}{UA + Q\,\rho c} \qquad (3.1)$$

$$Z_d = \frac{F_d + A\,S\,(1+\beta)}{UA_d + Q\,\rho c} \qquad (4.1)$$

$$Z_n = \frac{F_n + A\,S\,(1-2\beta)}{UA_n + Q\,\rho c} \qquad (4.2)$$

where: β is the solar apportioning factor.

The solar apportioning factor, β, indicates how much of the daily solar gain is utilized during the day (6^{oo} - 22^{oo}) and how much during the night (22^{oo} - 6^{oo}). For light buildings, β=0.5, which is equivalent to assuming that all solar energy is used during the 16 daylight hours. In massive houses, β=0, indicating that the incoming solar energy is assumed to be evenly spread over 24 hours. The factor 2 in the second equation is related to the ratio between 16 day hours and 8 night hours.

A schematic representation of the calculation of dynamic degree-days as applied to the heating season can be seen in Fig. 1. The calculation begins at 6^{oo} on January 1, with the temperature, T, equal to the night thermostat setpoint. At this hour the thermostat is reset to the daytime setting, which causes the heating system to operate continuously until the temperature rises to the day thermostat setpoint. Dynamic degree-days are accumulated during this reheat period, as indicated in Fig. 1.

When the daytime setpoint is reached, intermittent heating begins and dynamic degree-days are accumulated in a manner similar to that used for variable degree-days. If the outdoor temperature or the solar gain or the free heat are high enough, the effective outdoor temperature may rise above the setpoint. In this case, the indoor temperature is left to float, according to the equation shown in the box labelled "daytime floating temperature." The indoor temperature is not allowed to float more than 5.6 K (10 ^{o}F) above the daytime setpoint; this constraint is based on the assumption that occupants will ventilate the house to prevent overheating.

At 22^{oo} hours, the temperature is left to float down to the night thermostat setpoint, if this is lower than the daytime setpoint. Whenever the effective outside temperature is below the night setpoint, degree-day accumulation proceeds in the same manner as during daytime. At 6^{oo} hours the following morning, the cycle resumes by resetting the thermostat to the daytime setpoint, and so forth, until, at the end of the month, the totals for dynamic degree-days are stored and the

An inspection of the equations in Fig. 1 shows that dynamic degree-days are mainly dependent on the following parameters:

$T_{d,n}$: Day, night thermostat setting (^{o}C);
$Z_{d,n}$: Day, night temperature offsets through internal gains (K);
τ: Time constant (day).

As an illustration, dynamic degree-days for a few combinations of these parameters are plotted in Fig. 2. We compute monthly dynamic degree-days for many combinations of the same parameters prior to the field audit and store the results on floppy disk for retrieval during the actual audit.

Equivalent solar aperture and solar flux calculations

In computing average solar gains for each month, we make use of the concept of equivalent solar aperture, previously defined in an experimental study of simplified building models.[4] Simply stated, the solar aperture of a house is defined as the area of a south-facing, 100% transparent window that would allow the same amount of solar heat gain as the combination of actual windows and walls facing all compass directions. The solar aperture is evaluated month by month using the following equation:

$$A = \sum_i SC_i OC_i AW_i \left(\frac{S_i}{S}\right) + \sum_j \left(\frac{UA_j}{h_o}\right) \alpha_j \left(\frac{S_j}{S}\right)$$

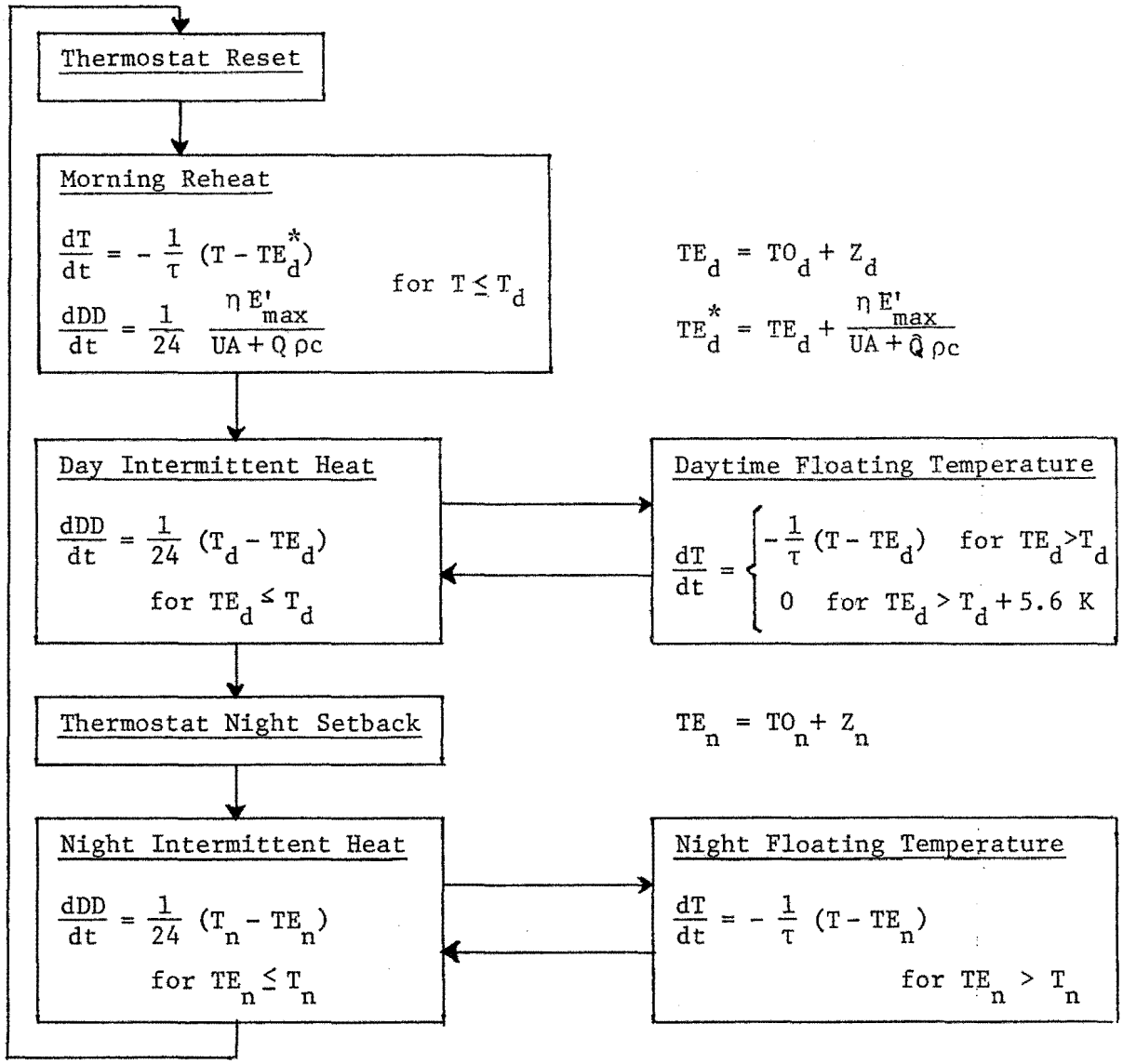

T = Inside temperature

$T_{d,n}$ = Day, night thermostat setting

$Z_{d,n}$ = Day, night temperature offset

$TE_{d,n}$ = Day, night effective outside temperature

E'_{max} = Maximum heating system input capacity

Fig. 1: SCHEMATIC REPRESENTATION OF DYNAMIC DEGREE-DAY CALCULATION

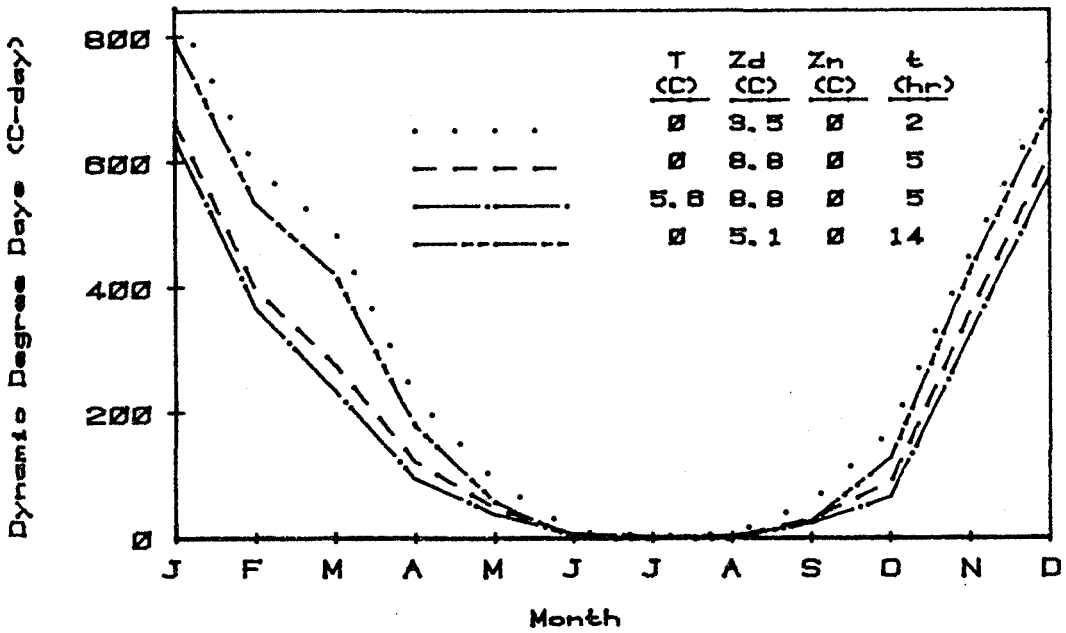

FIG. 2: MONTHLY DYNAMIC DEGREE DAYS Minneapolis

where: SC_i is the shading coefficient of the i-th window;
OC_i is the overhang coefficient of the i-th window;
AW_i is the area of the i-th window (m^2);
S_i is the total solar flux in the direction of window i (kWh/day);
S is the total solar flux on a south vertical surface (kWh/day);
UA_j is the heat transmission coefficient of the j-th wall (kWh/^{o}C-day);
h_o is the outside film coefficient (kWh/^{o}C-day);
α_j is the absorptivity of the j-th wall surface.

Shading coefficients are calculated from window data; overhang coefficients are calculated only for glass surfaces facing within $\pm 45^o$ of south, using correlations developed at the Los Alamos Scientific Laboratory.[3] Similar correlations were used to modify the shading coefficient for those daytime hours when the sun is not exactly south, and for modifying south solar fluxes when the house is not aligned precisely along a principal compass direction. Again, these corrections are applied only for glass within $\pm 45^o$ of south. Solar fluxes are calculated using measured total horizontal and diffuse fluxes for the same years for which the temperature data were used to calculate dynamic degree-days. The algorithm used to find the corresponding fluxes on all compass directions is a modified Liu-Jordan procedure as described by Kusuda.[5]

Comparison with DOE 2.1

We compared the heating consumptions calculated by our model to version 2.1 of the U.S. Department of Energy building simulation program.[6] The comparison was done for a simple house having several different thermal properties: high and low heat transmission and air infiltration, large and small solar aperture, high and low thermal mass. Night thermostat setbacks were 0 K, 2.8 K (5 °F), and 5.6 K (10 °F). The resulting 24 combinations were tried in four different cities, representing several climatic zones in the United States: Washington D.C., Minneapolis MN, Albuquerque NM, San Francisco CA. Table 1 shows a summary of the assumed building parameters.

Table 1: House Parameters used in comparing CIRA to DOE 2.1

Case	UA+Qρc [kWh/C-day]	C [kWh/C]	τ [hr]	A [m^2]	α
1	3.50	2.77	19	13.4	0
2	8.76	2.92	8	13.4	0
3	3.50	0.73	5	13.4	0.5
4	8.76	0.73	2	13.4	0.5
5	3.02	7.31	58	6.7	0
6	10.32	7.31	17	6.7	0
7	3.02	1.76	14	6.7	0.5
8	8.33	1.73	5	6.7	0.5

Table 2 shows conventional degree-days and horizontal total solar fluxes for the four cities.

Table 2: Climatic data on 4 cities used in comparison

City	Heating DD base 18.3°C (°C-day)	Cooling DD base 21.1°C (°C-day)	Annual Avg. Horiz. Solar (kWh/m^{2}-day)
Washington DC	2360	526	3.89
Minneapolis	4691	341	3.45
Albuquerque	2554	512	5.28
San Francisco	2058	38	4.60

In Figs. 3-6 we compare heating loads calculated on the basis of dynamic degree-days (labelled CIRA, for "Computerized Instrumented Residential Audit") and equation 1 to the results obtained from DOE 2.1. Again we emphasize that this is a comparison between an hour-by-hour load procedure (DOE 2.1) and a monthly average technique (CIRA). Also plotted are heating loads calculated on the basis of variable degree-days. Cases 1 and 5 in Table 1 (energy-efficient, massive house with high and low solar aperture) are plotted in Fig. 3. Cases 2 and 6 (wasteful, massive house with high and low solar aperture) are plotted in Fig. 4, and so forth. The axis labels are logarithmic, because of the large range of energy consumption across cities and configurations. The solid line in each plot indicates perfect correspondence. The dashed lines parallel to the solid line indicate ±20% discrepancy between simplified methods and DOE 2.1. Note that the largest discrepancies are for very low consumption levels (less than 300 kWh/Mo), where solar and internal gains nearly cancel the losses by conduction and infiltration. These points contribute very little to the annual totals. For higher consumption levels, the correspondence is generally within 10%.

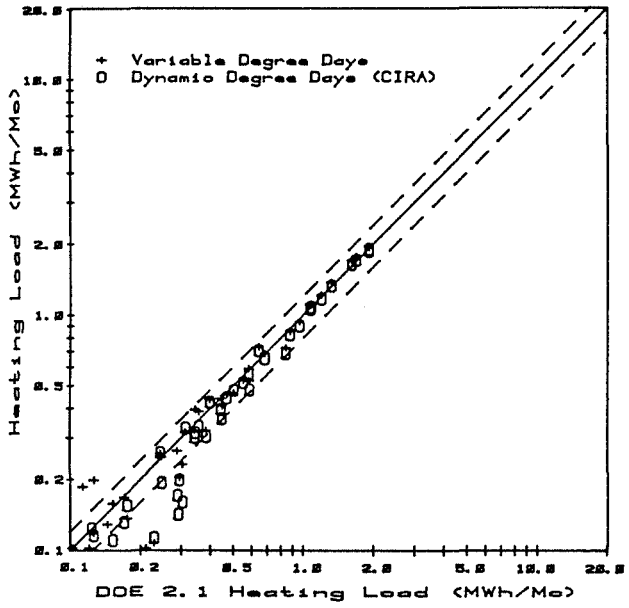

FIG. 3: DOE2.1 vs. SIMPLIFIED METHODS.
Four cities.
UA+Qpo= 3.2 kWh/C-day.
Solar aperture= 4.7 & 9.4 sq.m.
Massive. No setback.

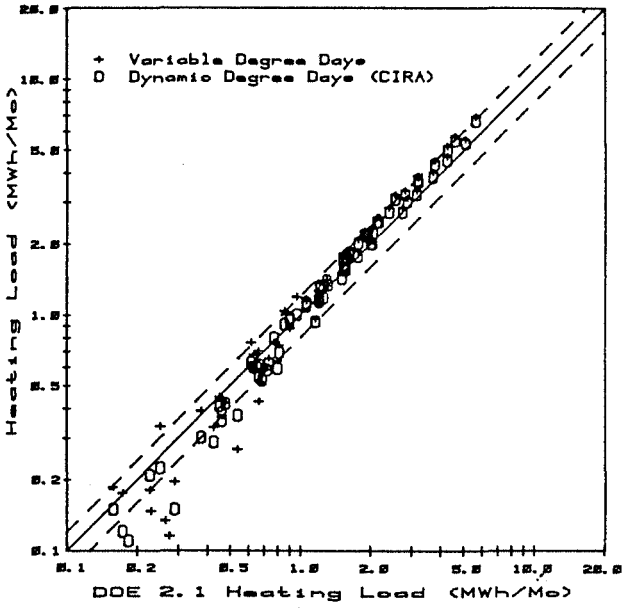

FIG. 4: DOE2.1 vs. SIMPLIFIED METHODS.
Four cities.
UA+Qpo= 9.0 kWh/C-day.
Solar aperture= 4.7 & 9.4 sq.m.
Massive. No setback.

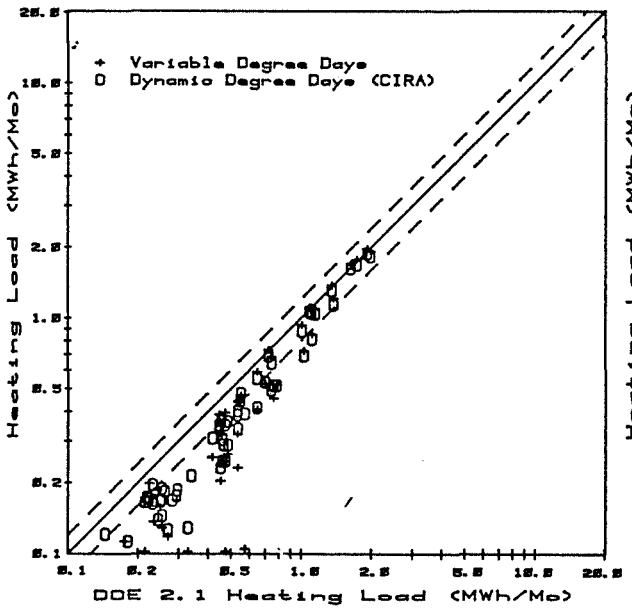

FIG. 5: DOE2.1 vs. SIMPLIFIED METHODS.
Four cities.
UA+Qpo= 3.2 kWh/C-day.
Solar aperture= 4.7 & 9.4 sq.m.
Light. No setback.

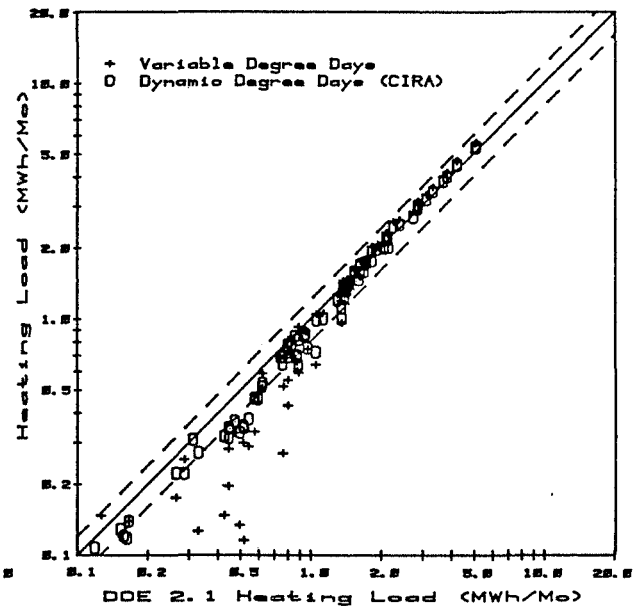

FIG. 6: DOE2.1 vs. SIMPLIFIED METHODS.
Four cities.
UA+Qpo= 9.0 kWh/C-day.
Solar aperture= 4.7 & 9.4 sq.m.
Light. No setback.

Table 3 compares annual total consumptions calculated with DOE 2.1 and CIRA. Agreement is generally best for energy-wasting houses that have large annual consumption levels. Discrepancies between CIRA and DOE 2.1 are highest in San Francisco, which has an unusual climate that is least suitable for this kind of simplified model.

Comparisons among the results obtained through dynamic degree-days (labelled CIRA), variable degree-days, and DOE 2.1., for a 5.6 K (10 ^{o}F) thermostat night setback, are shown in figures 7-10. The pattern of discrepancy is similar as for the case of no setback, but the

Table 3: CIRA & DOE 2.1 annual totals (MWh/Yr) -- NO setback

Mass	H*	A	WASH. DC DOE2	WASH. DC CIRA	MINNEAPOLIS DOE2	MINNEAPOLIS CIRA	ALBUQUERQUE DOE2	ALBUQUERQUE CIRA	S. FRANCISCO DOE2	S. FRANCISCO CIRA
Hi	Lo	Hi	2.96	2.21	9.37	8.82	1.50	0.93	0.68	0.08
Lo	Lo	Hi	4.73	2.99	10.87	9.17	4.07	2.88	3.25	1.99
Hi	Hi	Hi	13.69	13.21	30.79	31.78	11.98	11.87	9.01	6.72
Lo	Hi	Hi	14.75	13.67	31.76	32.13	13.72	13.00	11.83	8.71
Hi	Lo	Lo	3.85	3.56	9.94	9.84	2.64	2.71	1.51	1.01
Lo	Lo	Lo	4.62	3.65	10.52	9.83	3.83	2.94	3.13	1.46
Hi	Hi	Lo	17.38	19.55	35.72	42.01	16.82	19.59	13.85	14.52
Lo	Hi	Lo	15.70	15.36	32.72	33.45	15.05	15.39	12.69	11.02

* $H = UA + Q \rho c$

differences are slightly higher. Table 4 shows a comparison of the annual consumption totals.

Table 4: CIRA & DOE 2.1 annual totals (MWh/Yr) -- 5.6 K setback

Mass	H*	A	WASH. DC DOE2	WASH. DC CIRA	MINNEAPOLIS DOE2	MINNEAPOLIS CIRA	ALBUQUERQUE DOE2	ALBUQUERQUE CIRA	S. FRANCISCO DOE2	S. FRANCISCO CIRA
Hi	Lo	Hi	2.35	2.33	8.27	8.68	1.11	1.19	0.48	0.20
Lo	Lo	Hi	3.97	2.38	9.54	8.37	3.07	2.26	2.07	1.50
Hi	Hi	Hi	11.12	12.08	27.54	29.93	9.54	10.80	5.84	6.01
Lo	Hi	Hi	11.88	11.28	28.25	29.35	10.91	10.44	7.59	4.89
Hi	Lo	Lo	3.25	3.89	8.95	10.25	2.14	3.13	1.14	1.39
Lo	Lo	Lo	3.78	3.60	9.42	9.58	3.03	3.17	2.19	2.09
Hi	Hi	Lo	14.79	18.92	32.25	40.74	14.14	19.19	10.06	13.81
Lo	Hi	Lo	12.97	13.55	29.36	31.42	12.39	13.54	8.50	7.32

* $H = UA + Q \rho c$

Based on the results of these comparisons, we feel confident in using dynamic degree-days for estimating energy savings. It should be emphasized that these comparisons were done with little optimization of parameters such as the time constant and the solar apportioning factor. Some research remains to be done to determine the best values for different configurations of a house.

Infiltration

Infiltration, the uncontrolled leakage of air into a house, is a sizeable fraction of the energy load of that structure. Although several standard techniques exist to measure infiltration in a building,[7] few of these techniques are applicable for an energy audit because of the limitations in time inherent in such a procedure. The time constraint forces us to adopt either a short, cursory examination of the structure to give information about infiltration or to use an indirect measurement procedure using fan pressurization. The simplicity and speed of the pressurization procedure and the quality of the infiltration predictions obtainable with this technique favor the use of this procedure in the audit.

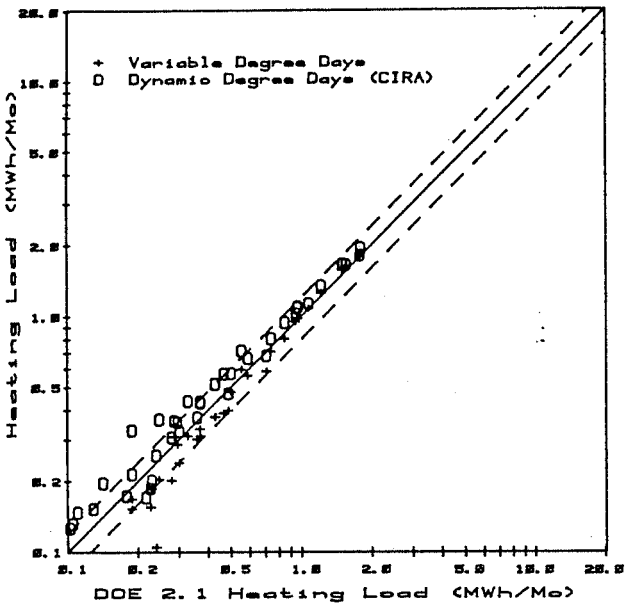

FIG. 7: DOE2.1 vs. SIMPLIFIED METHODS.
Four cities.
UA+Qpo= 3.2 kWh/C-day.
Solar aperture= 4.7 & 9.4 sq.m.
Massive. 5.6 C setback.

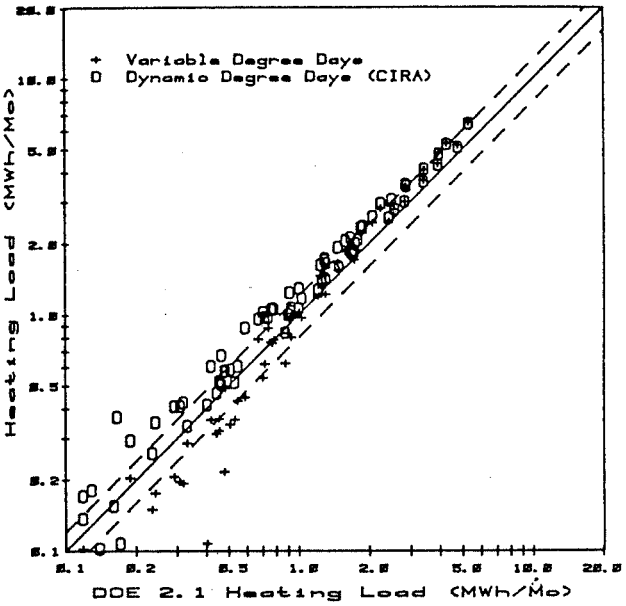

FIG. 8: DOE2.1 vs. SIMPLIFIED METHODS.
Four cities.
UA+Qpo= 9.0 kWh/C-day.
Solar aperture= 4.7 & 9.4 sq.m.
Massive. 5.6 C setback.

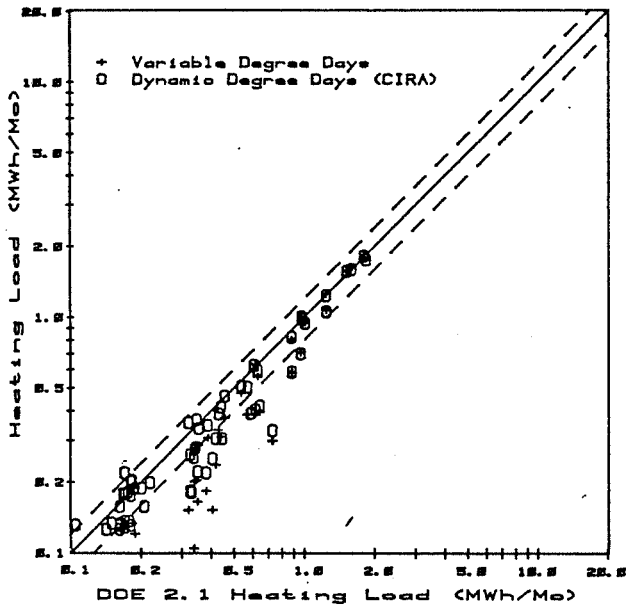

FIG. 9: DOE2.1 vs. SIMPLIFIED METHODS.
Four cities.
UA+Qpo= 3.2 kWh/C-day.
Solar aperture= 4.7 & 9.4 sq.m.
Light. 5.6 C setback.

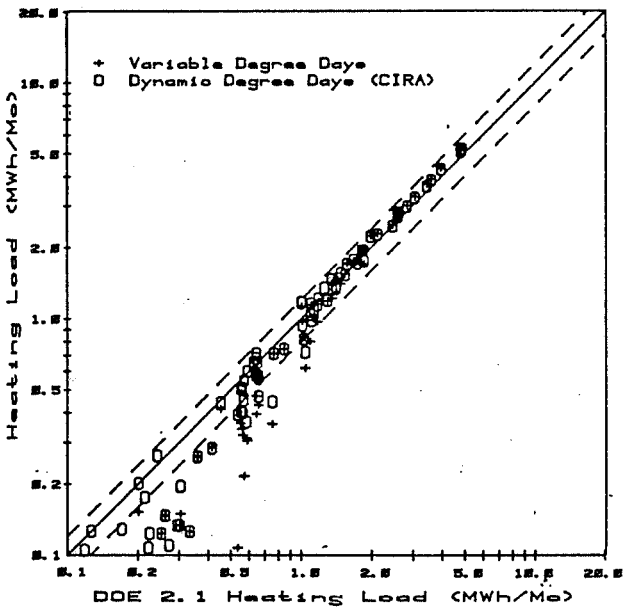

FIG. 10: DOE2.1 vs. SIMPLIFIED METHODS.
Four cities.
UA+Qpo= 9.0 kWh/C-day.
Solar aperture= 4.7 & 9.4 sq.m.
Light. 5.6 C setback.

Pressurization and leakage area

During pressurization, a fan mounted on an adjustable wooden plate is sealed into a doorway of the house to be tested. The fan speed, which can be adjusted using a DC motor and controller, is varied to produce a pressure drop, ΔP, across the building envelope. The flow through the fan, required to produce this pressure difference, is determined by means of a previously established fan calibration curve that expresses flow as a function of RPM and pressure drop. This process is repeated for fixed pressure increments to produce a curve relating the pressure drop across the envelope to the flow required to produce it. The fan direction is reversed and a corresponding curve of depressurization

versus flow is obtained in the same manner.

The flows at equal positive and negative pressures are averaged. In the pressure region used ($\pm$ 10 to $\pm$ 60 Pa) the data generally are well represented by the empirical relationship

$$Q = K \Delta P^n \tag{6}$$

where: Q is the volume flow rate through the fan (m^3/s);
K is a constant;
ΔP is the absolute value of the pressure drop across the building envelope (Pa);
n is an exponent in the range $0.5 < n < 1.0$

The curve is then extrapolated toward the low-pressure end of the graph to determine the flow at 4 Pa (a pressure of this order is typical of the pressures that drive natural infiltration). Now the assumption is made that in the low-pressure regime in the vicinity of 4 Pa the pressure-flow relationship has the form of inviscid flow through large openings, i.e.,

$$Q = L \sqrt{\frac{2}{\rho} \Delta P} \qquad \text{for } \Delta P \simeq 4 \text{ Pa} \tag{7}$$

where: L is the effective leakage area (m^2);
ρ is the density of air (kg/m^3).

This expression, in turn, is used to compute the effective leakage area.

The leakage area of a house, L, is used as a measure of the tightness of the structure. We shall see in the next section how it can be related to air infiltration. Our assumption of inviscid flow around 4 Pa and, thus, our definition of leakage area, rests on measurements of the air flow through a house at very low pressures using a technique we call AC pressurization.[8]

Figure 11 shows a graphical approach for finding the leakage area of a house. During a field pressurization test, the auditor notes the RPM of the fan at several specific pressure differences, then converts these RPM readings to air-flow readings with the help of the fan calibration curves traced in the left half of the figure. In the right half he plots each measured point, with its pressure difference as the abscissa and the corresponding air flow as the ordinate. Since the axes are both logarithmic, the points should lie approximately along a straight line. The best-fitting straight line is extrapolated to 4 Pa and yields the leakage area of the house.

Two sample curves are traced in Fig. 11: the upper set of points was measured in a house before retrofit; the lower half was measured after six hours of sealing leaks, caulking cracks and inserting gaskets in electrical fixtures. The leakage area decreased from 1,250 cm^2 to 625 cm^2.

We have found it useful to normalize leakage area by floor area. Most houses will fall somewhere between 2 and 20 cm^2/m^2, with the tight houses below 5 cm^2/m^2. In the next section we will discuss how such measurements of leakage area are transformed into monthly air

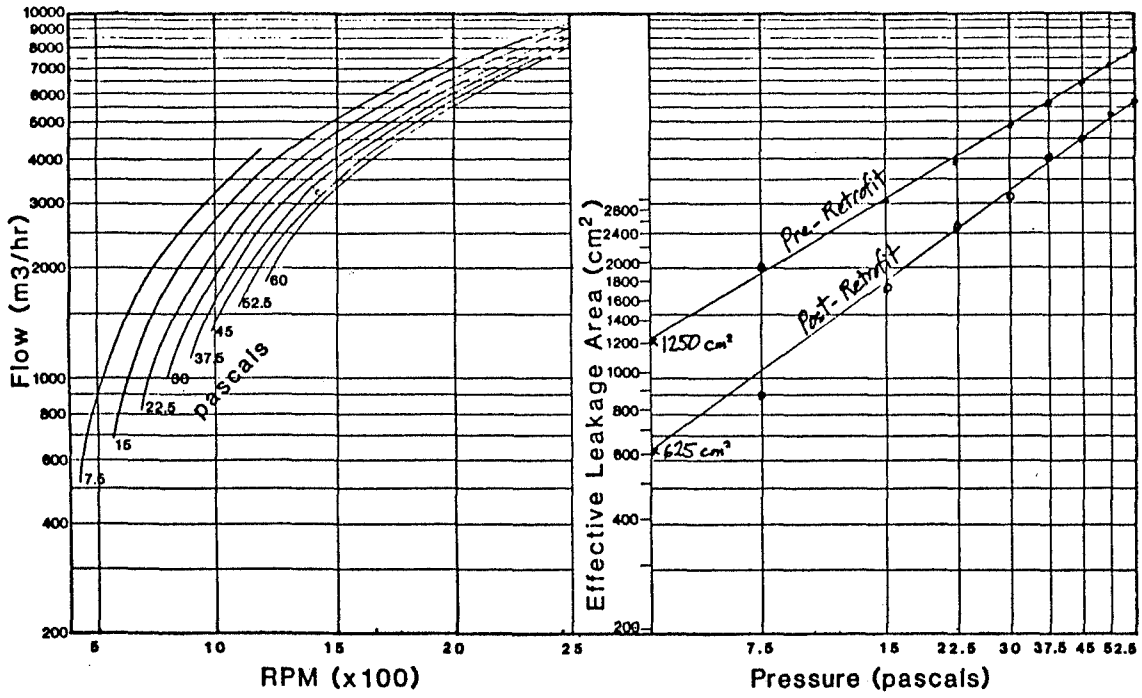

FIG.11 GRAPHICAL PROCEDURE TO DETERMINE LEAKAGE AREA

infiltration rates.

Air Infiltration Model

The model used in our audit to calculate air infiltration from leakage area, terrain features and weather, has been described previously.[9] Briefly, specific air infiltration (volumetric air infiltration rate per unit leakage area) is calculated as a superposition of stack and wind-induced components, according to the equation:

$$\frac{Q}{L} = \sqrt{\left[\frac{Q_{stack}}{L}\right]^2 + \left[\frac{Q_{wind}}{L}\right]^2} \qquad (8)$$

where

$$\frac{Q_{stack}}{L} = f_s \sqrt{\Delta T} \qquad (9.1)$$

$$\frac{Q_{wind}}{L} = f_w v \qquad (9.2)$$

$$L = \frac{Q}{\sqrt{2\frac{\Delta P}{\rho}}} \qquad \text{where } \Delta P \simeq 4 \text{ Pa} \qquad (9.3)$$

The leakage area, L, has been described in the previous section. The stack infiltration component is proportional to the square root of the average indoor-outdoor temperature difference. The wind component is proportional to the wind speed measured at the nearest weather tower. The coefficients of proportionality, f_s and f_w, are the reduced stack and wind parameters, respectively. Both depend on the building height and the leakage distribution; the reduced wind parameter depends

additionally on the local terrain features:

$$f_s = \frac{1 + R/2}{3} \left[1 - \frac{X^2}{(2-R)^2}\right]^{3/2} \sqrt{\frac{gH_h}{T}} \qquad (10.1)$$

$$f_w = C' \, (1 - R)^{1/3} \left[\frac{\alpha_h (H_h/10)^{\gamma_h}}{\alpha_w (H_w/10)^{\gamma_w}}\right] \qquad (10.2)$$

where: H_h is the grade-to-ceiling height of the house (m);
g is the acceleration of gravity (9.81 m/s^2);
T is the absolute indoor temperature (293 K);
C' is the local shielding coefficient;
α_h, γ_h describe the terrain class near the house;
α_w, γ_w describe the terrain class where the wind measurements are made;
H_w is the height of the wind measuring tower (m);
R, X describe the leakage area distribution.

The parameters describing leakage area distribution are defined as:

$$R = \frac{L_{ceil} + L_{floor}}{L} \qquad (11.1)$$

$$X = \frac{L_{ceil} - L_{floor}}{L} \qquad (11.2)$$

where: L_{ceil} is the ceiling leakage area (cm^2);
L_{floor} is the floor leakage area (cm^2).

The term in brackets in the definition of f_w "translates" the wind pattern at the weather/tower site to the wind pattern at the building site. The terrain classes at the two sites are determined on the basis of large-scale topographical features, such as hills, developments and forests. Table 5a lists the parameters α,γ for the five different terrain classes used in wind-engineering applications.

Table 5a: Terrain parameters for standard terrain classes

Class	γ	α	Description
I	0.10	1.30	Ocean or other body of water with at least 5 km of unrestricted expanse
II	0.15	1.00	Flat terrain with some isolated obstacles (e.g. buildings or trees well separated from each other
III	0.20	0.85	Rural areas with low buildings, trees, etc.
IV	0.25	0.67	Urban, industrial or forest areas
V	0.35	0.47	Center of large city (e.g. Manhattan)

The shielding coefficient, C′, is determined on the basis of local topographical features, such as nearby trees and fences. Five shielding classes have been tentatively established and are listed in Table 5b.

Table 5b: Generalized shielding coefficient vs. local shielding

Shielding Class	C′	Description
I	0.324	No obstructions (trees, fences, nearby houses) whatsoever
II	0.285	Light local shielding with few obstructions
III	0.240	Some obstructions within two house heights
IV	0.185	Obstructions around most of perimeter
V	0.102	Large obstruction surrounding perimeter within two house heights

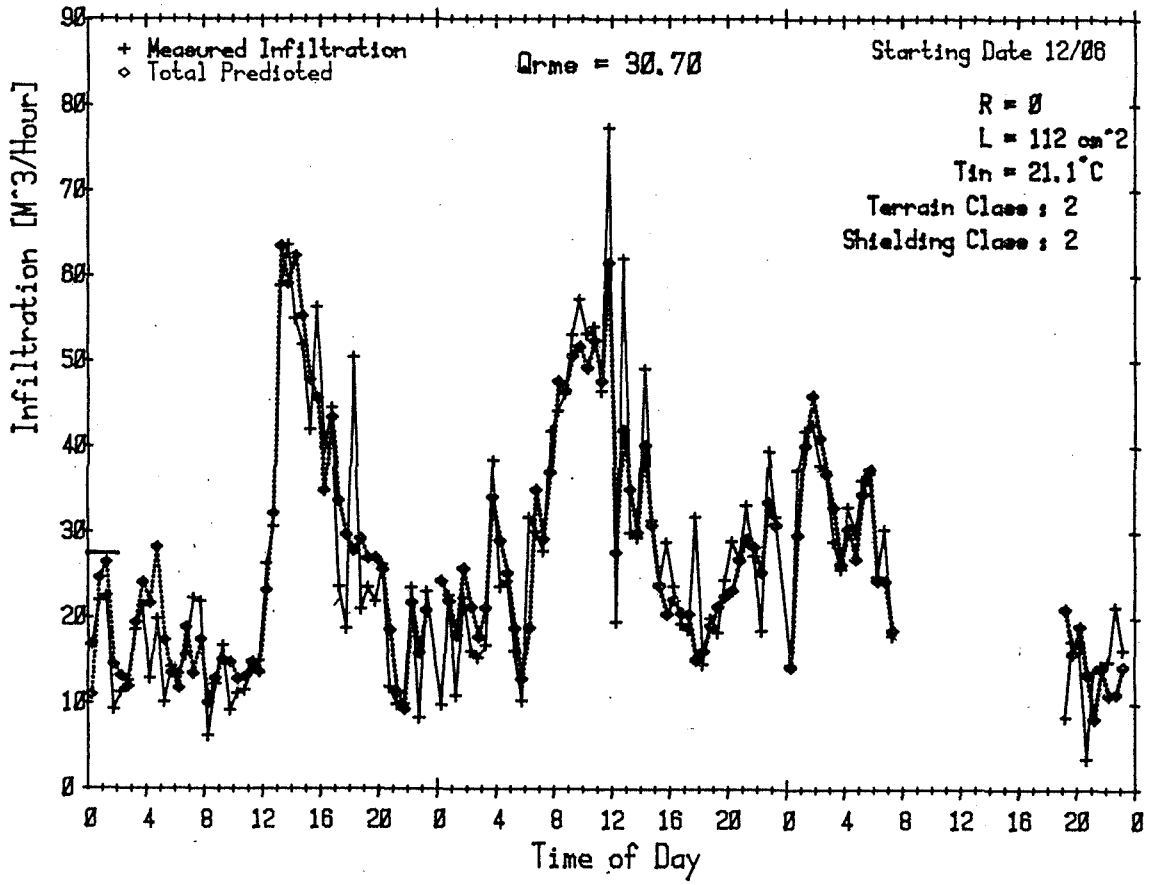

Fig 12. AIR INFILTRATION vs TIME

An example of the ability of the model to predict infiltration on a short term basis is shown in Fig. 12. Here, we use a three-day data set recently measured by our Mobile Infiltration Test Unit (MITU), a trailer outfitted with adjustable leaks and cracks, pressure sensors and weather station used for detailed field investigations of air infiltration phenomena. The solid line shows infiltration measurements obtained using a controlled flow injection system. The discrete measurement results, represented by crosses, are obtained at half-hour intervals over the three-day period shown. The dotted line represents the

infiltration predicted for this structure using the model described above. The average infiltration for this structure over the measurement period shown is 27.0 m^3/hr. The average computed using our model is 27.3 m^3/hr.

Another validation of the infiltration model using 15 different houses located in California, Minnesota, Iowa, New Jersey and Canada has been reported earlier.[9] Predictions for those houses generally fell within ± 15% of the values measured with standard tracer gas techniques.

Application of infiltration model to audit

On the basis of our infiltration model, we have developed a procedure simple enough to be used by auditors with relatively little technical training. In this application we use the concept of a reference house in reference surroundings. The reference house is a single-story building (height=2.5m) with average leakage distribution (R=0.5; i.e., ceiling and floor leakage areas together are equal to the wall leakage area). By reference surroundings we mean terrain class III (rural areas with low buildings and trees) and shielding class III (some obstructions within two house heights). We then calculated monthly values of specific infiltration for the reference house in reference surroundings for 59 cities, using weather tapes for Test Reference Years (TRY-tapes). Table 6 shows seasonal averages of wind and stack components as well as total specific infiltration and resulting heat load.

It is interesting to note that the variation in infiltration per-unit-leakage area across the U.S. is relatively small for this reference case. The variation is typically a factor of two for stack-driven infiltration and a factor of three for wind-driven infiltration.

Corrections for non-reference cases

For houses or surroundings different from the reference case, we must apply appropriate corrections by means of the following equations:

$$\frac{Q^{act}_{stack}}{L} = cf_s \frac{Q^{ref}_{stack}}{L} \qquad (12.1)$$

$$\frac{Q^{act}_{wind}}{L} = cf_w \frac{Q^{ref}_{wind}}{L} \qquad (12.2)$$

where: act refers to the actual values;
ref refers to the values for the reference case;
cf_s is the correction factor for the stack term;
cf_w is the correction factor for the wind term.

$$cf_s = 0.253\ (1 + R/2) \left[1 - \frac{X^2}{(2-R)^2}\right]^{3/2} \sqrt{H_h} \qquad (13.1)$$

$$cf_w = 8.15\ c_h (H_h/10)^{y_h}\ C'\ (1 - R)^{1/3} \qquad (13.2)$$

Table 6: Seasonal Specific Infiltration ($m^3/hr/cm^2$) in 59 US cities

City	$\frac{Q_{stack}}{L}$	$\frac{Q_{wind}}{L}$	$\frac{Q}{L}$	City	$\frac{Q_{stack}}{L}$	$\frac{Q_{wind}}{L}$	$\frac{Q}{L}$
Albany, NY	.21	.23	.31	Medford OR	.18	.10	.21
Albuquerque	.18	.17	.24	Memphis TN	.15	.21	.26
Amarillo TX	.17	.30	.35	Miami FL	.0	.20	.20
Atlanta GA	.15	.22	.26	Minneapolis	.23	.23	.32
Bismarck ND	.24	.23	.33	Nashville TN	.16	.22	.27
Boise ID	.19	.20	.27	New Orleans	.12	.22	.25
Boston MA	.19	.32	.37	New York NY	.17	.27	.32
Brownsville	.05	.26	.27	Norfolk VA	.15	.26	.31
Buffalo NY	.20	.29	.35	Oklahoma Ci.	.17	.32	.36
Burlington	.21	.22	.31	Omaha NE	.20	.23	.31
Charleston	.13	.21	.25	Philadelphia	.18	.26	.32
Cheyenne WY	.20	.29	.35	Phoenix AX	.12	.10	.16
Chicago IL	.19	.22	.29	Pittsburgh	.19	.19	.27
Cincinnati	.18	.20	.27	Raleigh NC	.16	.21	.26
Cleveland OH	.20	.25	.32	Richmond VA	.18	.19	.26
Columbia MO	.18	.22	.29	Sacramento	.16	.14	.21
Detroit MI	.20	.26	.33	Salt Lake C.	.20	.18	.27
Dodge City	.19	.29	.35	San Antonio	.12	.21	.25
El Paso TX	.15	.19	.24	San Diego CA	.11	.15	.19
Fort Worth	.14	.25	.29	S. Francisco	.14	.19	.24
Fresno CA	.14	.12	.19	Seattle WA	.17	.22	.28
Gr't Falls	.21	.36	.42	St. Louis MO	.19	.24	.30
Houston TX	.12	.25	.27	Tampa FL	.06	.21	.21
Indianapol	.19	.24	.31	Tulsa OK	.16	.24	.29
Kansas City	.19	.23	.3,	Washing. DC	.17	.17	.24
Lake Charles	.12	.21	.24	Jacksonville	.10	.20	.23
Los Angeles	.11	.17	.20	Jackson MS	.14	.22	.26
Louisville	.18	.23	.29	Portland ME	.21	.19	.28
Lubbock TX	.16	.30	.34	Portland OR	.17	.23	.29
Madison WI	.21	.21	.30				

To summarize, infiltration measurements in the context of an instrumented energy audit can be made quickly and accurately by using the fan pressurization technique. The measurement provides a value of the effective leakage area of the structure. In addition, particular leakage sites can easily be identified by using smoke sticks or other air flow pattern detectors. The technique is direct, uses simple equipment and provides measurement values that can be analyzed simply in the field to find the infiltration.

Conclusions

A successful audit procedure imposes special constraints on procedures and instrumentation. Accuracy, brevity, simplicity and minimal expense are general goals that direct the development of any audit. The procedures described in this report represent particular solutions that combine recent advances in instrumentation and modeling to yield fast, reliable results using relatively inexpensive equipment. The interaction of the homeowner with the audit team is an important element of this audit. This will inform the homeowner both about proper operation of the house and also encourage implementation of the recommendations of the audit.

In this paper we have concentrated on technical aspects of our audit. The results are encouraging, but much work remains to be done to improve the accuracy of our simplified heat load model and to extend it to predict cooling consumption.

Many additional problems require investigation. The issue of indoor air quality is present whenever retrofits are proposed that decrease the infiltration in a structure. Long-term field tests must be completed that realistically account for costs and allow adequate evaluation of savings. Institutional problems of delivery of the audit and retrofit services must be solved. Each is an interesting problem in its own right; solutions will contribute to all building energy projects.

References

1. T. Kusuda, I. Sud and T. Alereza, "Comparison of DOE-2 Generated Residential Design Energy Budgets with those Calculated by the Degree-day and Bin Methods," ASHRAE Trans. 87(1), 1981.

2. A. Dupagne, H. Heikhaus, J. Lebrun, J. Uyttenbroeck, "Practical Method to Evaluate the Effect of Building Characteristics in the Energy Needs for Heating," Presented at the Intl. Congress on Building Energy Management, Póvoa de Varzim, Portugal, May 12-16, 1980.

3. J. D. Balcomb et al., "Passive Solar Design Handbook, Volume Two," National Technical Information Service DOE/CS-0127/2, Springfield, Virginia, 1980.

4. R. Sonderegger, "Diagnostic Methods to Determine the Thermal Response of a House," ASHRAE Trans. 84(1), 1978, and Lawrence Berkeley Laboratory report, LBL-6856 (1977).

5. T. Kusuda and K. Ishii, "Hourly Solar Radiation Data for Vertical and Horizontal Surfaces on Average Days in the United States and Canada," National Bureau of Standards, Building Science Series 96, April 1977.

6. M. Lokmanhekim et al., "DOE-2: A New State-of-the-Art Computer Program for the Energy Utilization Analysis of Buildings," Proc. 2nd Intl. CIB Symposium on Energy Conservation in the Built Environment, Copenhagen, Denmark, May/June 1979. Lawrence Berkeley Laboratory report LBL-8974 (1979).

7. M. H. Sherman, D. T. Grimsrud, P. E. Condon and B. V. Smith, "Air Infiltration Measurement Techniques," Proc. Air Infiltration Centre Symposium on Instrumentation and Measuring Techniques, Windsor, UK, Oct 6-8, 1980, and Lawrence Berkeley Laboratory report, LBL-10705 (1980).

8. M. H. Sherman, D. T. Grimsrud and R. C. Sonderegger, "The Low Pressure Leakage Function of a Building," Proc. ASHRAE-DOE Conf. on The Thermal Performance of the Exterior Envelope of Buildings, Orlando, FL, Dec 1979. Lawrence Berkeley Laboratory report, LBL-9162 (1979).

9. M. H. Sherman, D. T. Grimsrud, "Measurement of Infiltration Using Fan Pressurization and Weather Data," Proc. Air Infiltration Centre Symposium on Measurement Techniques, Windsor, UK, Oct 6-8, 1980, and Lawrence Berkeley Laboratory report, LBL-10852 (1980).

DISCUSSION

L. LARET : in your transient heat balance equation, you compute hour by hour. For solar effects terms, you use hourly solar radiation. Do your take into account hourly, and yearly varying solar aperture ?

R. SONDEREGGER : solar apertures for five orientations are re-computed monthly.

A. REGEF :which assumption can be made on the effect of opening the windows with very tight houses with poor specific ventilation devices ?

R. SONDEREGGER : open windows can be modeled as increases in leakage area of the house. However, our air infiltration model will be the less accurate, the more the leakage area is concentrated on a few discrete openings. As far as I know, no general theory exists yet to model the effect of open windows on air infiltration.

R. RAYMENT : How easy is cost information included in energy audits ?

R. SONDEREGGER : because of the data base-type of structure in CIRA, input and updating of cost information is very easy. Unfortunately, the uncertainty of the cost data remains, especially where innovative retrofits are concerned, but this is an issue unrelated to CIRA.

J.E. WOODS : does your energy audit procedure require the use of the pressure door tests? If not, what is expected of the auditor in obtaining appropriate data ?

R. SONDEREGGER : pressure door tests are desirable, but not required by CIRA. When direct pressurisation data are not available, leakage areas are computed component-by-component. In general, the auditor only has to enter the number of light fixtures, vents, windows and electrical outlets. Default leakage areas are programmed into the audit to convert these entries into reasonable estimates of leakage areas.

A. BOYSEN :Fig. 12 Air infiltration vs time shows the correlation for an extremely tight building with the effective leakage area L as low as 112 cm^2. What is the correlation measured/ predicted infiltration for more normal buildings ?

R. SONDEREGGER : tests have been done on 15 houses located throughout the U.S. and Canada. Comparisons of predictions based on effective leakage area and measurements based on tracer gas techniques are shown in the two figures below. Leakage areas vary from 100 to 1600 cm^2. The dashed lines indicate our $\pm$ 15% measurement accuracy. Houses n° 10, 15 and 14 are "underpredicted" because of the absence of dampers in their fireplace chimneys.

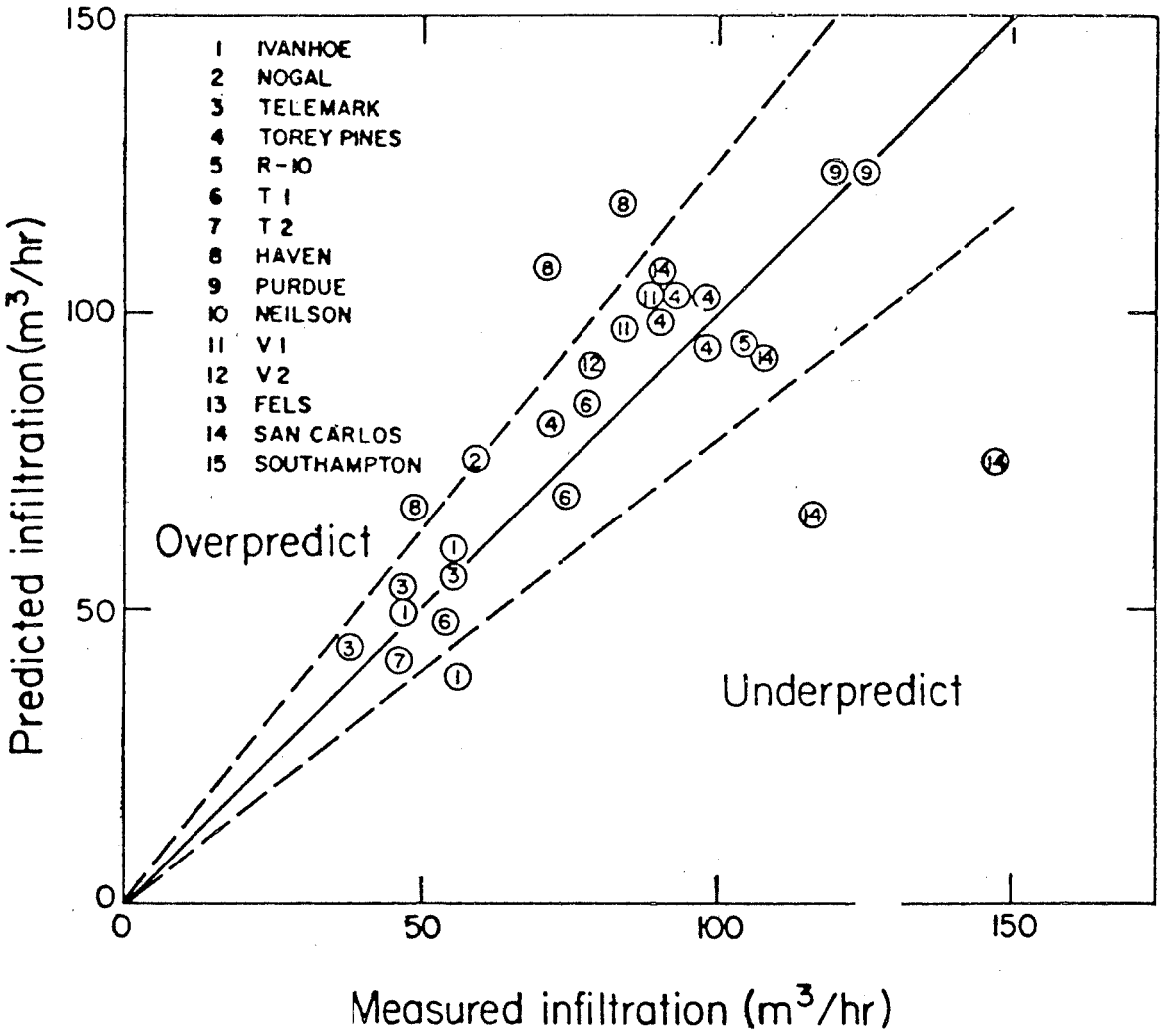
1 IVANHOE
2 NOGAL
3 TELEMARK
4 TOREY PINES
5 R-10
6 T 1
7 T 2
8 HAVEN
9 PURDUE
10 NEILSON
11 V 1
12 V 2
13 FELS
14 SAN CARLOS
15 SOUTHAMPTON
Overpredict
Underpredict
Predicted infiltration (m³/hr)
Measured infiltration (m³/hr)
0
50
100
150

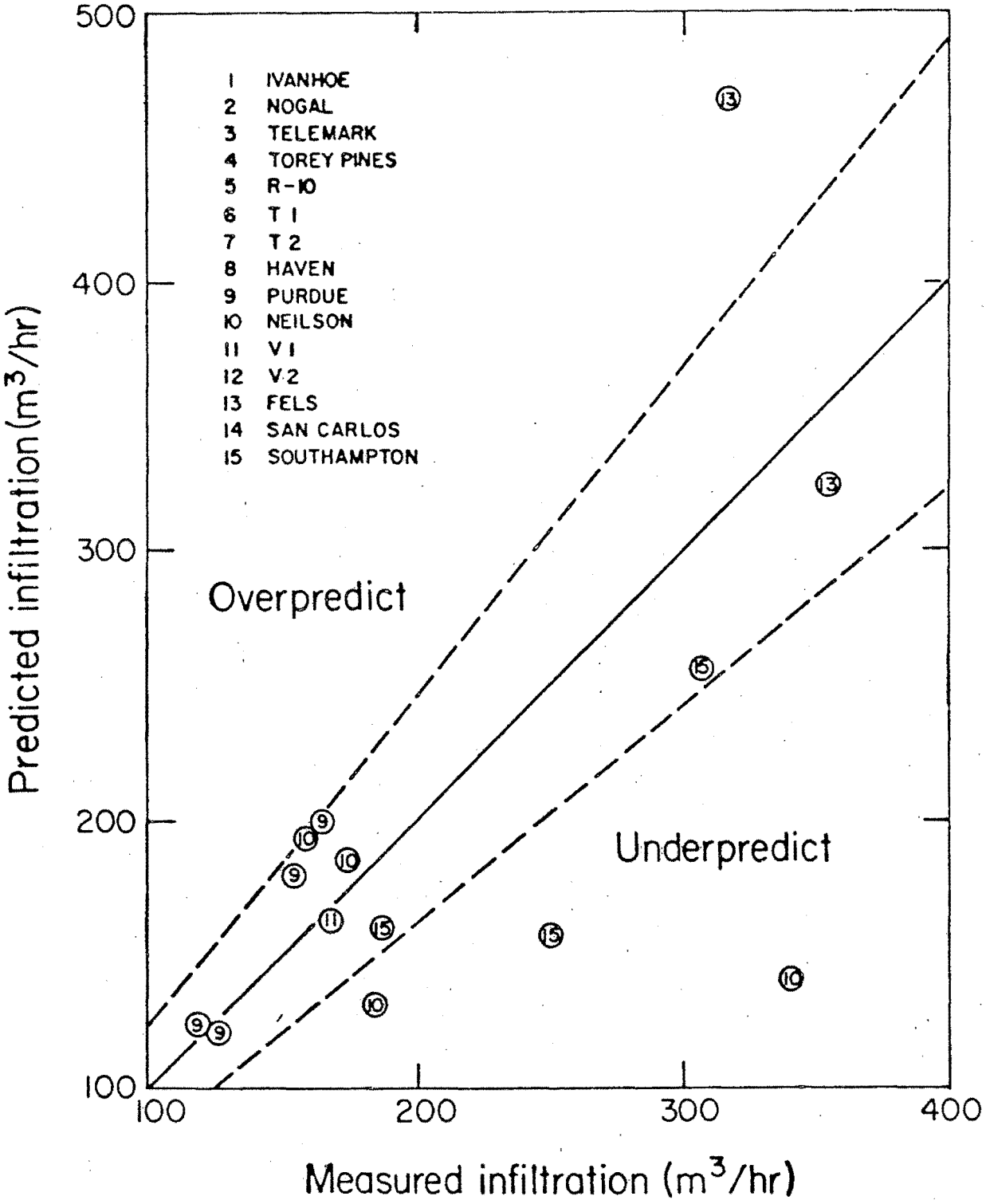
1 IVANHOE
2 NOGAL
3 TELEMARK
4 TOREY PINES
5 R-10
6 T 1
7 T 2
8 HAVEN
9 PURDUE
10 NEILSON
11 V 1
12 V 2
13 FELS
14 SAN CARLOS
15 SOUTHAMPTON
Overpredict
Underpredict
Predicted infiltration (m³/hr)
Measured infiltration (m³/hr)
100
200
300
400
500

P. NUSGENS : about air infiltration, you have very fine results without taking into account the wind direction. Do you think that it is always true, especially when the house has most windows to the south , the main wind direction being from North-West ?

R. SONDEREGGER : as you correctly point out, the predictions of our model are the more inaccurate, the less uniform the leakage distribution over the envelope of the house. In such cases, our model tends to "overpredict" infiltration. However, in all but the most "flat" terrain and shielding classes, wind direction effects are sufficiently diffused by local, small scale turbulence, that we have so far found very few "pathological cases" as you describe above.